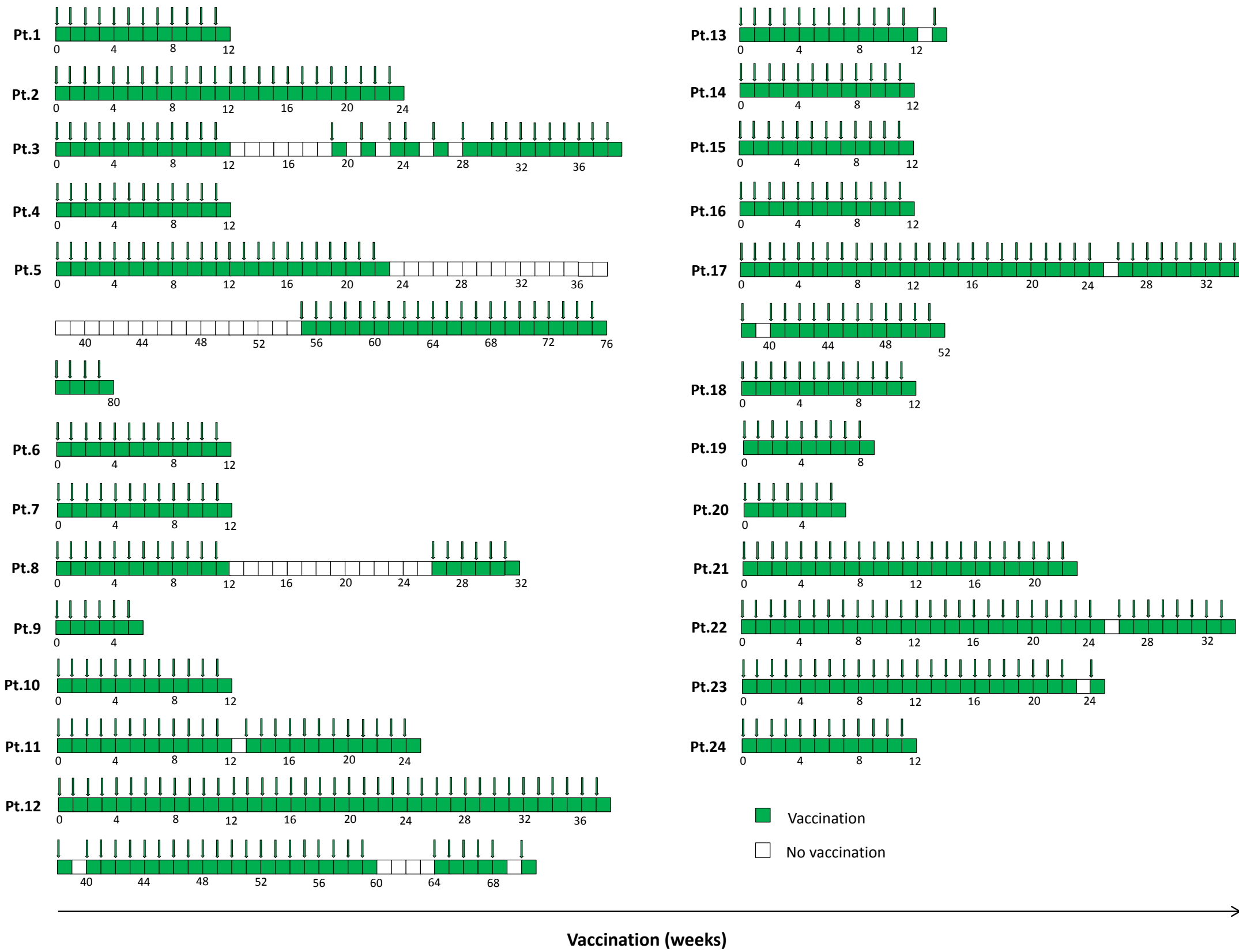

Fig. S1. Immunization time course of the 24 PPV patients. Each square represents one week. Green squares and arrows represent weeks when vaccination was received and white squares represent weeks when no vaccine was administered. According to the trial design, patients were to receive weekly vaccinations for a minimum of 12 weeks. All patients completed 12 weeks of vaccination, with the exception of Pts. 9, 19, and 20, who expired during the initial trial period due to advanced disease. Patients were given the opportunity to continue immunizations beyond 12 weeks if they desired.

a.

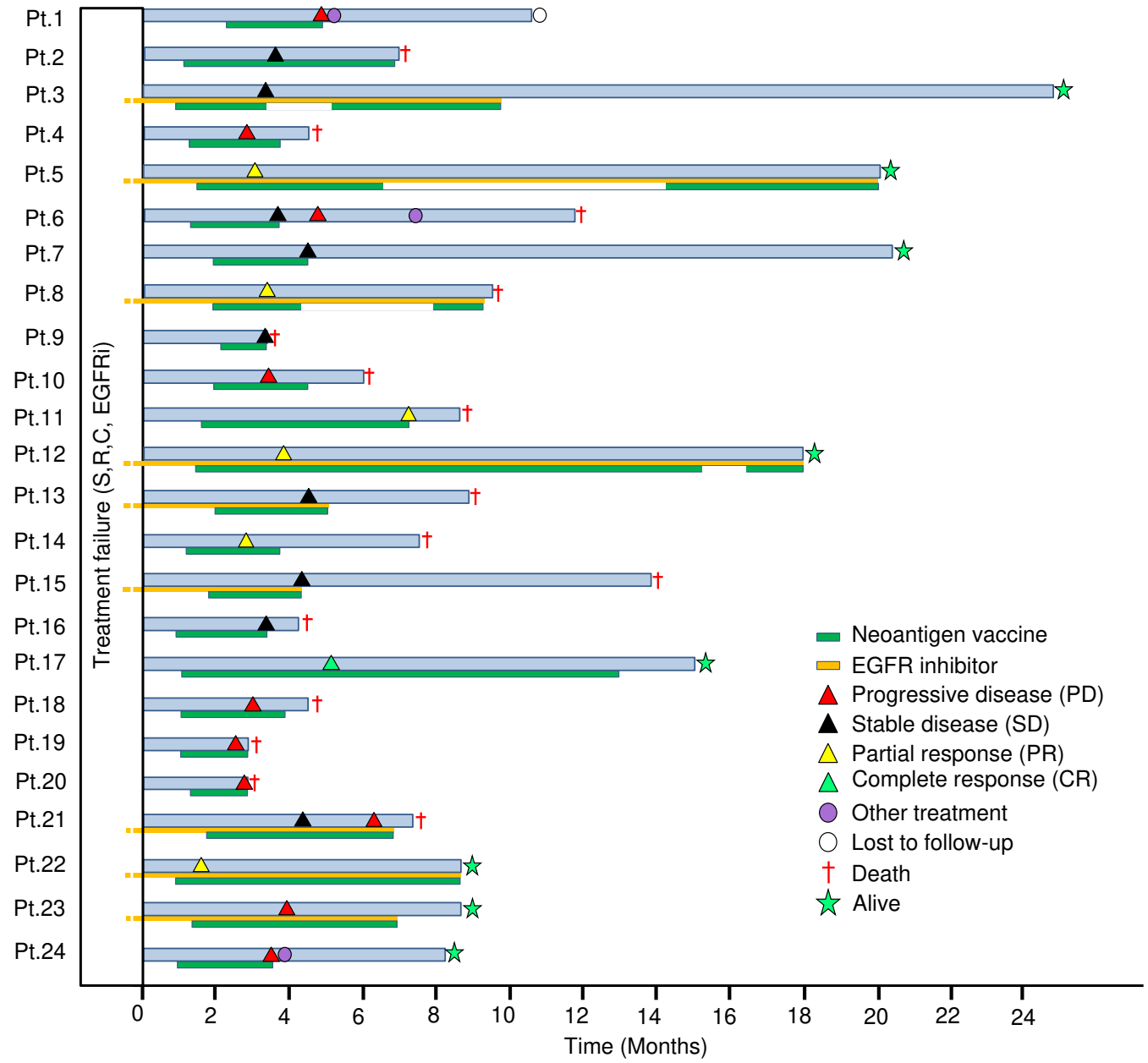

b.

Event	Grade 1 # of patients (%)	Grades 2-5 # of patients (%)
Fatigue	2 (9.5)	0
Rash	1 (4.8)	0
Fever	1 (4.8)	0

c.

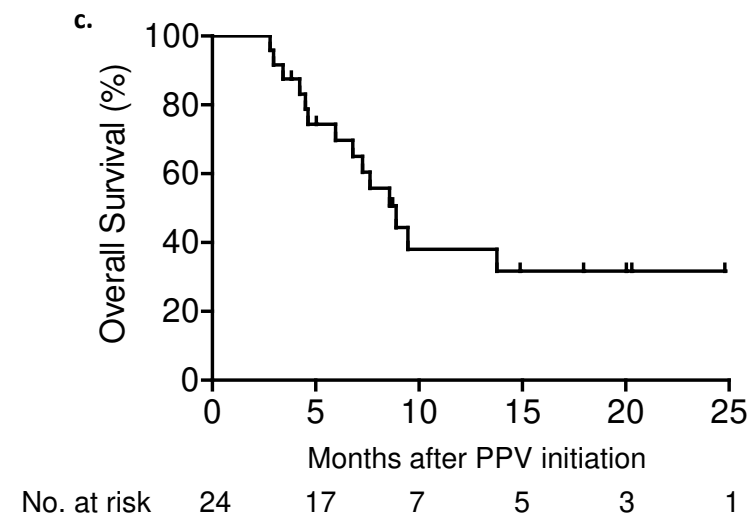

Fig. S2. **a.** Treatment and clinical outcomes of the 24 PPV patients. **b.** List of treatment-related adverse events. **c.** Overall survival curve of all PPV patients (n=24). Survival curve was generated using Kaplan-Meier estimate.

a. **Summary of clinical baseline characteristics by group**

Characteristic	PPV-1 *n=8*	PPV-2 *n=7*	PPV-3 *n=9*	P value *PPV-1 vs. PPV-2*	P value *PPV-1 vs. PPV-3*	P value *PPV2 vs. PPV-3*
Gender (Male-Female)	5-3	3-4	2-7	0.619	0.153	0.596
Age (year)	61.88 ± 11.08	61.14 ± 6.01	57.78± 10.39	0.879	0.444	0.496
Weight (kg)	63.13 ± 9.68	68.29± 9.98	65.75± 17.20	0.329	0.713	0.738
Height (cm)	166.80 ± 9.33	168.84± 8.32	162.40± 7.05	0.721	0.308	0.151
Smoke history (yes,%)	6 (75.0)	3 (42.9)	2 (22.2)	0.315	0.057	0.596
Pleural effusion (yes,%)	4 (50.0)	6 (85.7)	5 (55.6)	0.282	1.000	0.308
Tumor burden (cm)	4.93 ± 2.99	4.41± 1.17	4.39± 2.74	0.676	0.712	0.986
Tumor number (S-M)	2-6	2-5	1-8	1.000	0.577	0.550
EGFR mutation (yes,%)	0 (0)	7 (100)	9 (100)	-	-	-
Previous treatment strategies:						
Surgery (yes,%)	1 (12.5)	3 (42.9)	0 (0)	0.282	0.471	0.063
Radiotherapy (yes,%)	8 (100)	3 (42.9)	7 (77.8)	**0.026**	0.471	0.302
Chemotherapy (yes,%)	4 (50.0)	6 (85.7)	7 (77.8)	0.282	0.335	1.000
EGFR Inhibitor (yes,%)	0 (0)	7 (100)	9 (100)	-	-	-
Quality of life score	39.63 ± 10.51	40.43 ± 8.52	37.33 ± 8.43	0.875	0.625	0.480
Lymphocyte (%)	17.41 ± 8.77	22.16 ± 9.37	20.41 ± 10.10	0.330	0.536	0.736
Brian metastases (yes,%)	0 (0)	0 (0)	1 (11.1)	-	1.000	1.000
Tumor histology (SQ-AD)	5-3	1-6	0-9	0.119	**0.009**	0.438
EGFRi categories (1 – 2/3)	0-0	4-3	3-6	-	-	0.615
ECOG PS (0/1/2– 3)	6-2	6-1	7-2	1.000	1.000	1.000

b. **EGFR inhibitor treatment history of PPV patients**

Patient ID	First generation TKI (initiation - failure)	Second generation TKI (initiation - failure)	Third generation TKI (initiation - failure)	PPV initiation
PPV Group 2:				
Pt.11	Lcotinib (02/16 - 02/17)	No	No	07/2017
Pt.14	Erlotinib (07/16 - 08/17)	No	No	09/2017
Pt.16	Gefitinib (08/16 - 10/16)	No	No	12/2016
Pt.17	Lcotinib (05/16 - 03/17)	No	Osimertinib (04/17 - 09/17)	11/2017
Pt.18	Gefitinib (12/14 - 09/15)	No	Avitinib (09/15 - 03/16) Osimertinib (03/16 - 02/17)	06/2017
Pt.20	Gefitinib (07/16 - 10/17)	No	No	12/2017
Pt.24	Gefitinib (11/16 - 07/17)	Afatinib (10/17 - 11/17)	Osimertinib (07/17 - 04/18)	05/2018
PPV Group 3:				
Pt.3	Gefitinib (08/16 - 11/16)	No	No	01/2017
Pt.5	Erlotinib (12/15 - 09/16)	No	Osimertinib (01/17 - 04/17)	06/2017
Pt.8	Gefitinib (05/16 - 11/16)	No	Osimertinib (12/16 - 04/17)	06/2017
Pt.12	Gefitinib (11/16 - 05/17)	No	No	08/2017
Pt.13	Gefitinib (06/15 - 07/16)	No	Osimertinib (07/16 - 06/17)	09/2017
Pt.15	Gefitinib (08/13 - 11/14)	Afatinib (08/15 - 09/15)	Osimertinib (01/16 - 06/17)	09/2017
Pt.21	Gefitinib (03/17 - 01/18)	No	Osimertinib (01/18 - 02/18)	04/2018
Pt.22	Gefitinib (08/17 - 10/17)	No	Osimertinib (12/17 - 03/18)	05/2018
Pt.23	Gefitinib (05/17 - 03/18)	No	No	05/2018

Fig. S3. a. Summary of clinical baseline characteristics by group. Clinical and demographic characteristics of PPV groups at baseline are indicated, with statistical comparisons of groups PPV-1 (EGFR-WT, PPV only, n=8), PPV-2 (EGFR mutant, PPV only, n=7) and PPV-3 (EGFR mutant, PPV + EGFRi, n=9). S, single; M, multiple; SQ, squamous cell carcinoma; AD, adenocarcinoma. Continuous data were shown as mean± standard deviation (SD). Two-tailed unpaired *t* test or Chi-square test was used to analyze the statistical significance between groups. $P<0.05$ was considered significantly different. **b.** EGFR inhibitor treatment history of PPV-2 and PPV-3 patients. TKI, tyrosine kinase inhibitor.

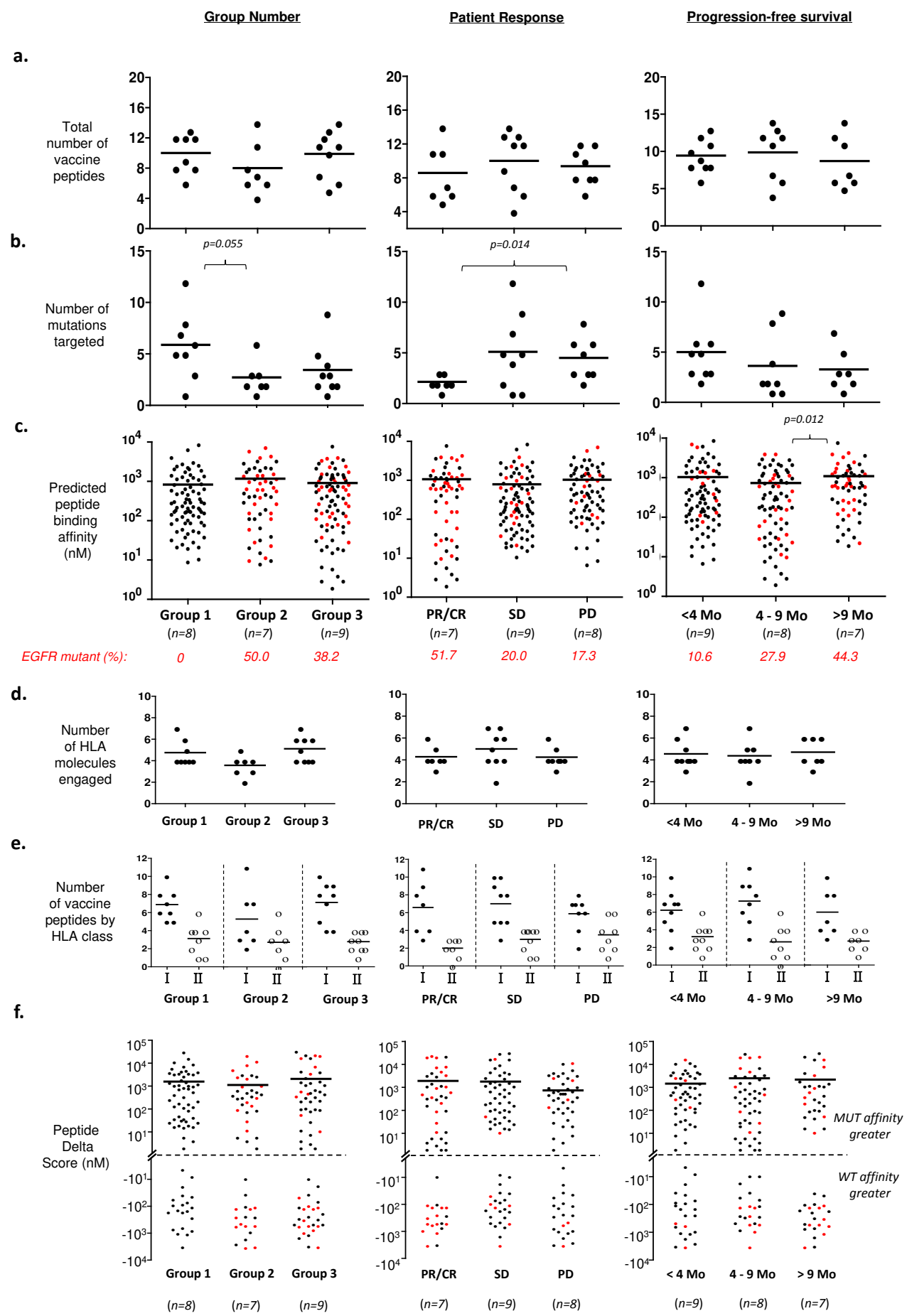

Fig. S4. Vaccine peptide analysis by group, clinical response and progression-free survival. a, b, c. Numbers of vaccine peptides, numbers of mutations targeted, and predicted vaccine peptide binding affinities stratified by patient group, clinical response and progression-free survival. Black dots indicate non-EGFR neoantigen peptides and red dots indicate EGFR neoantigen peptides, with percentages of the latter listed at bottom. **d.** Number of different HLA class I and class I molecules engaged by the vaccine peptides, as predicted by HLA peptide binding affinity. Each dot represents one PPV patient. **e.** Number of administered vaccine peptides restricted to HLA class I (short) or HLA class II (long). Each dot or circle represents one PPV patient. **f.** Peptide Delta Score of vaccine peptides. Delta Score is calculated by subtracting the mutant neoantigen peptide predicted binding affinity from the corresponding wild-type peptide binding affinity. Each dot represents one vaccine peptide. Red, EGFR neoantigen peptides; Black, non-EGFR neoantigen peptides. N number of each group was indicate in each graph. Using a two-way ANOVA test with multiple group comparison adjustment (Dunnett's test) or Z test, no significant differences were found between groups, with $P<0.05$ considered significantly different. MUT, mutated. WT, wild-type. PD, progressive disease; SD, stable disease; PR, partial response; CR, complete response.

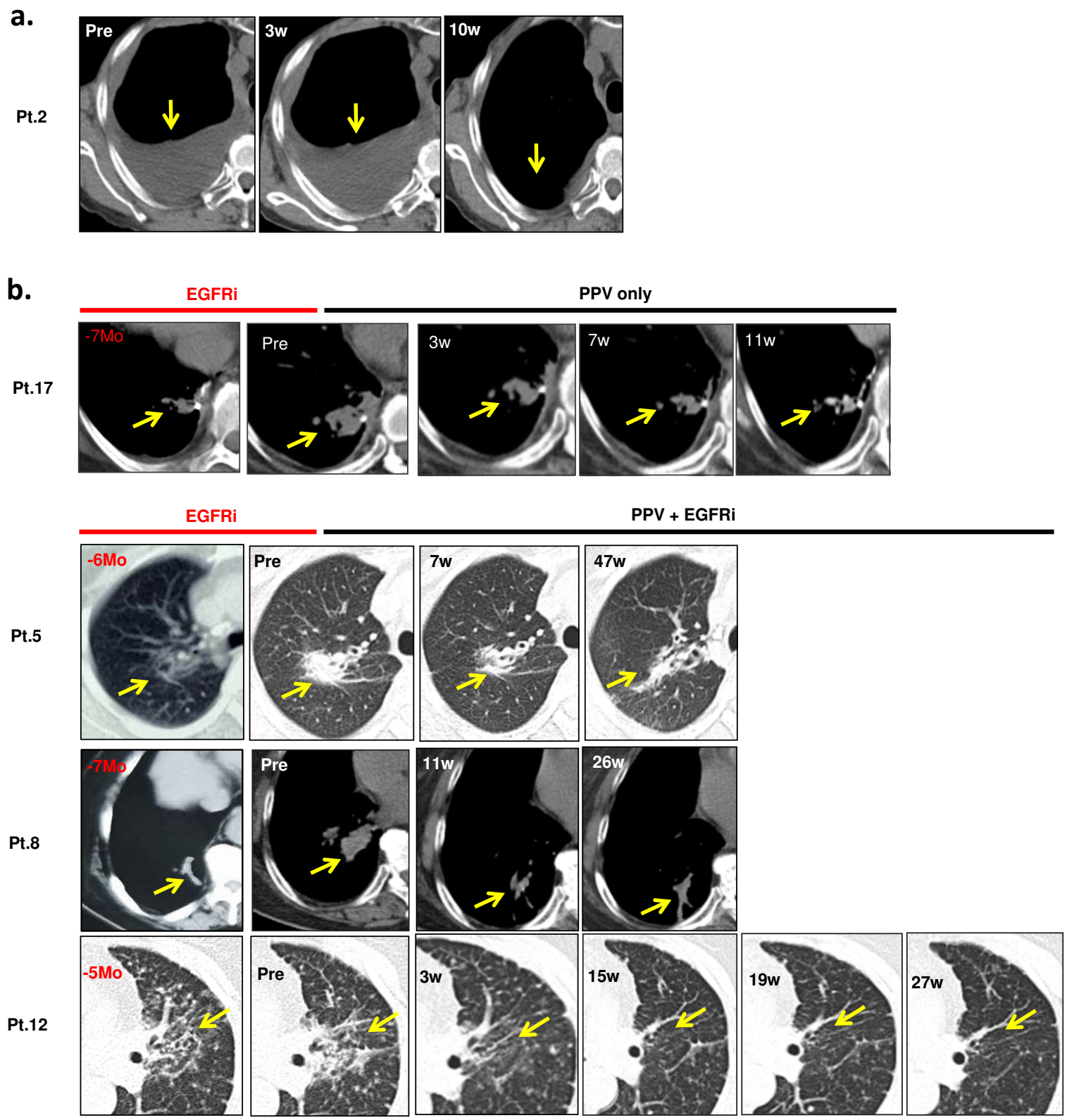

Fig. S5. Representative CT scans of selected PPV patients, including pre-vaccine trial EGFR inhibitor failures. a. Serial CT scans showing that pleural effusion of Patient 2 (Group 1) disappeared 10 weeks after PPV treatment. **b.** Serial CT scans depicting pre-PPV trial EGFR inhibitor failures in Patients 17, 5, 8 and 12 followed by clinical objective responses after starting PPV treatment.

a.

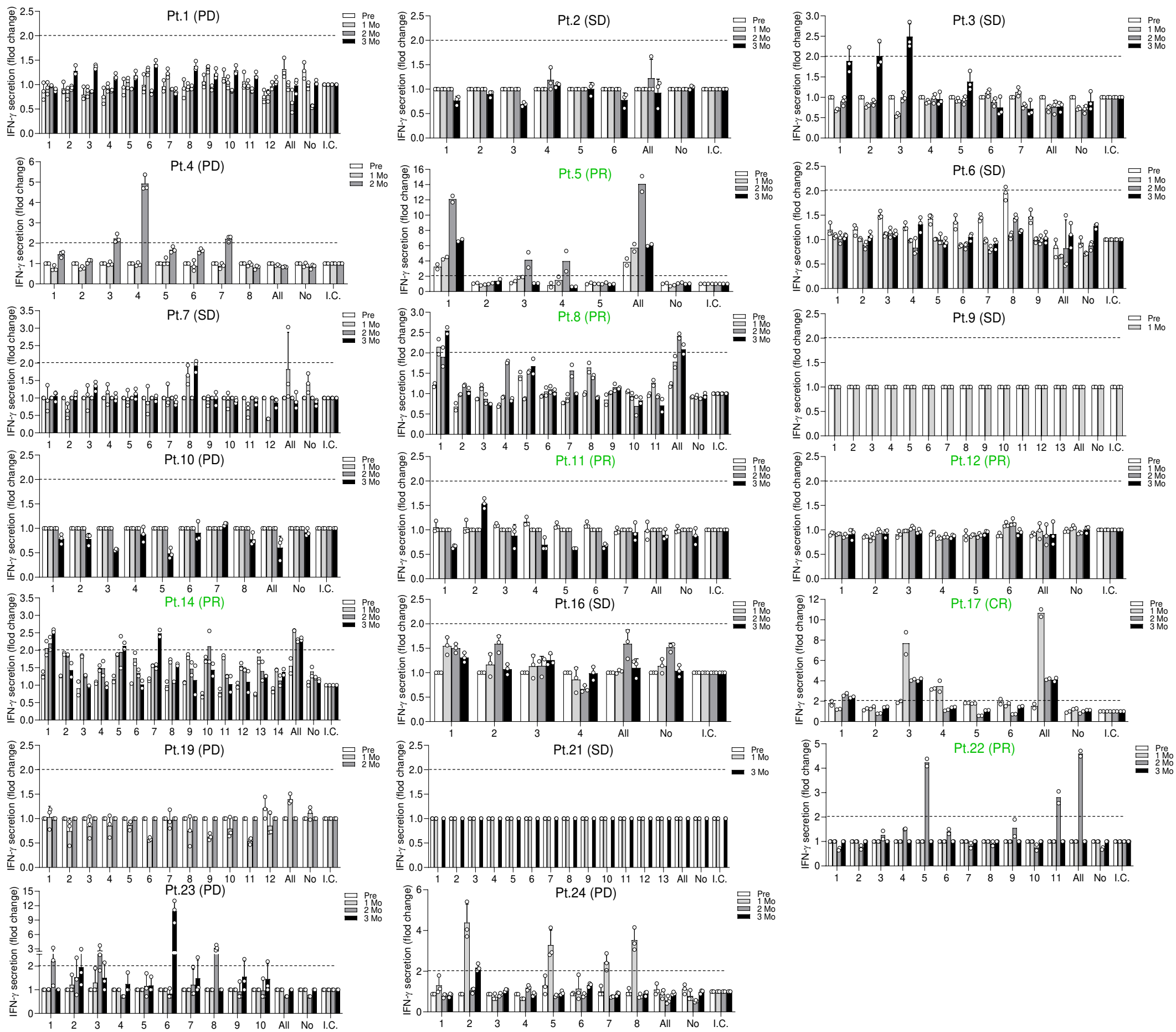

b.

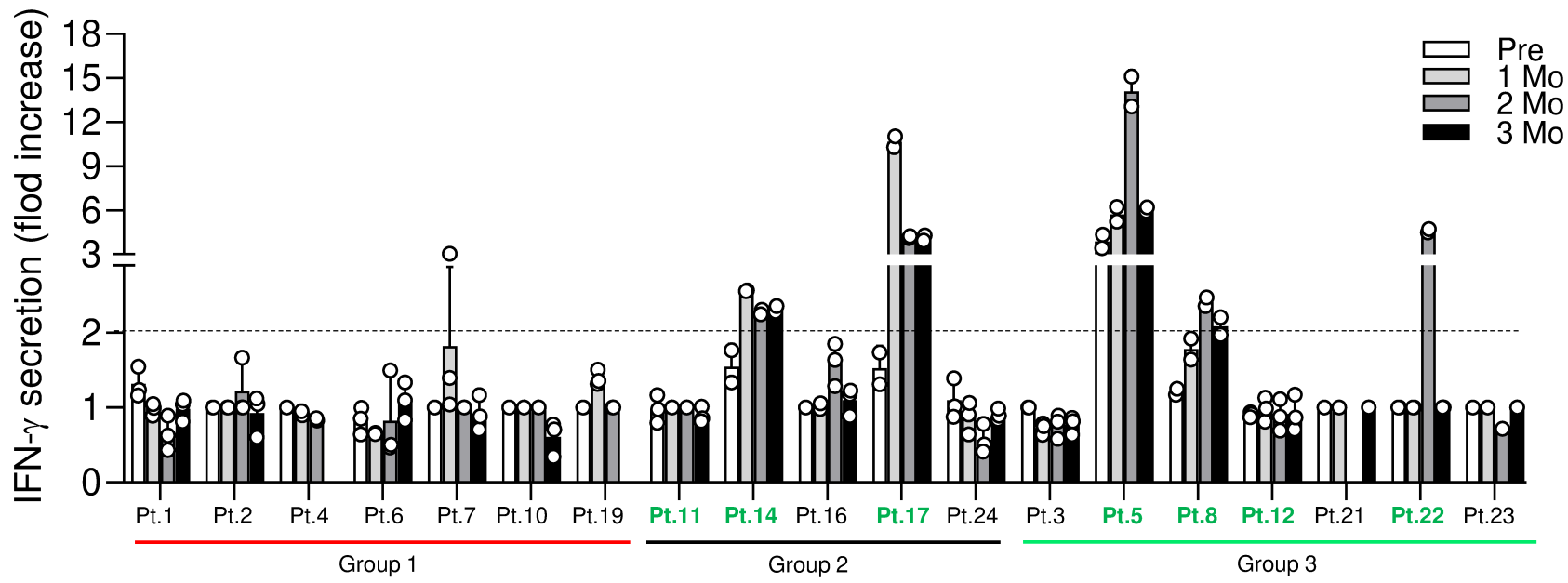

c.

Peptide category	Number of patients	Peptides admin-istered	Peptides eliciting response
All peptides	8	80	7
	5	39	15
	7	63	24
EGFR peptides	0	0	NA
	5	19	9
	7	25	12
TP53 peptides	6	15	1
	1	4	1
	2	11	5

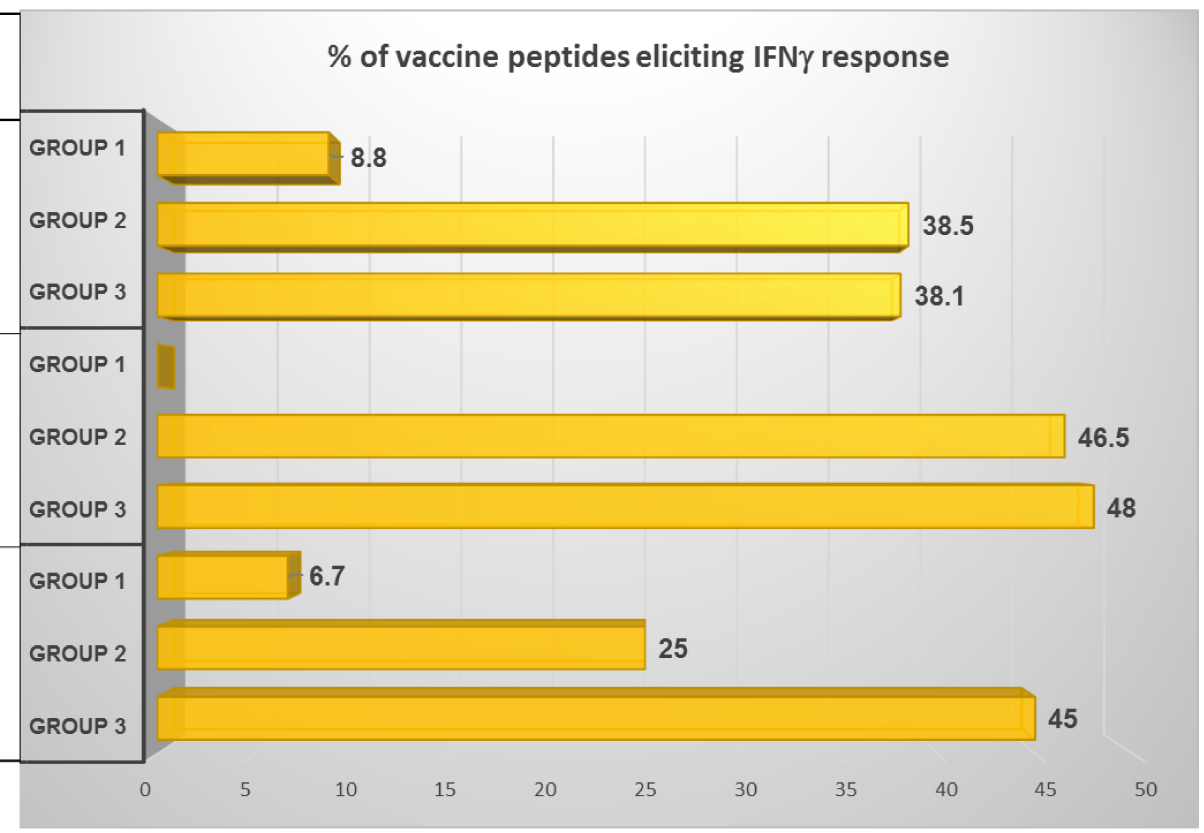

Fig. S6. ELISA-based immune monitoring of PPV-induced immune responses. a. Results of IFN-γ ELISA assay measuring peripheral blood reactivity in response to individual vaccine peptides. Peptide numbers correspond to those listed in Supplemental Table 2. Fold change is measured relative to the no peptide control (No) at the indicated time points. Experiment was performed once in n=2 or 3 replicates. I.C., irrelevant peptide control. Clinical responders are indicated in green font. **b.** Interferon-gamma (IFN-γ) ELISA assays performed on all peptide pool-stimulated patient PBMC supernatants showed vaccine peptide pool-specific responses primarily in 5 PPV patients: 5, 8, 14, 17 and 22. All five patients had experienced objective RECIST-based clinical responses following PPV (green). Experiment was performed once in n=2 or 3 replicates. **c.** Percentage of total vaccine peptides, EGFR peptides, and TP53 peptides shown to elicit a detectable neoantigen-specific immune response using at least one assay at one post-immunization time point, as divided by patient groups.

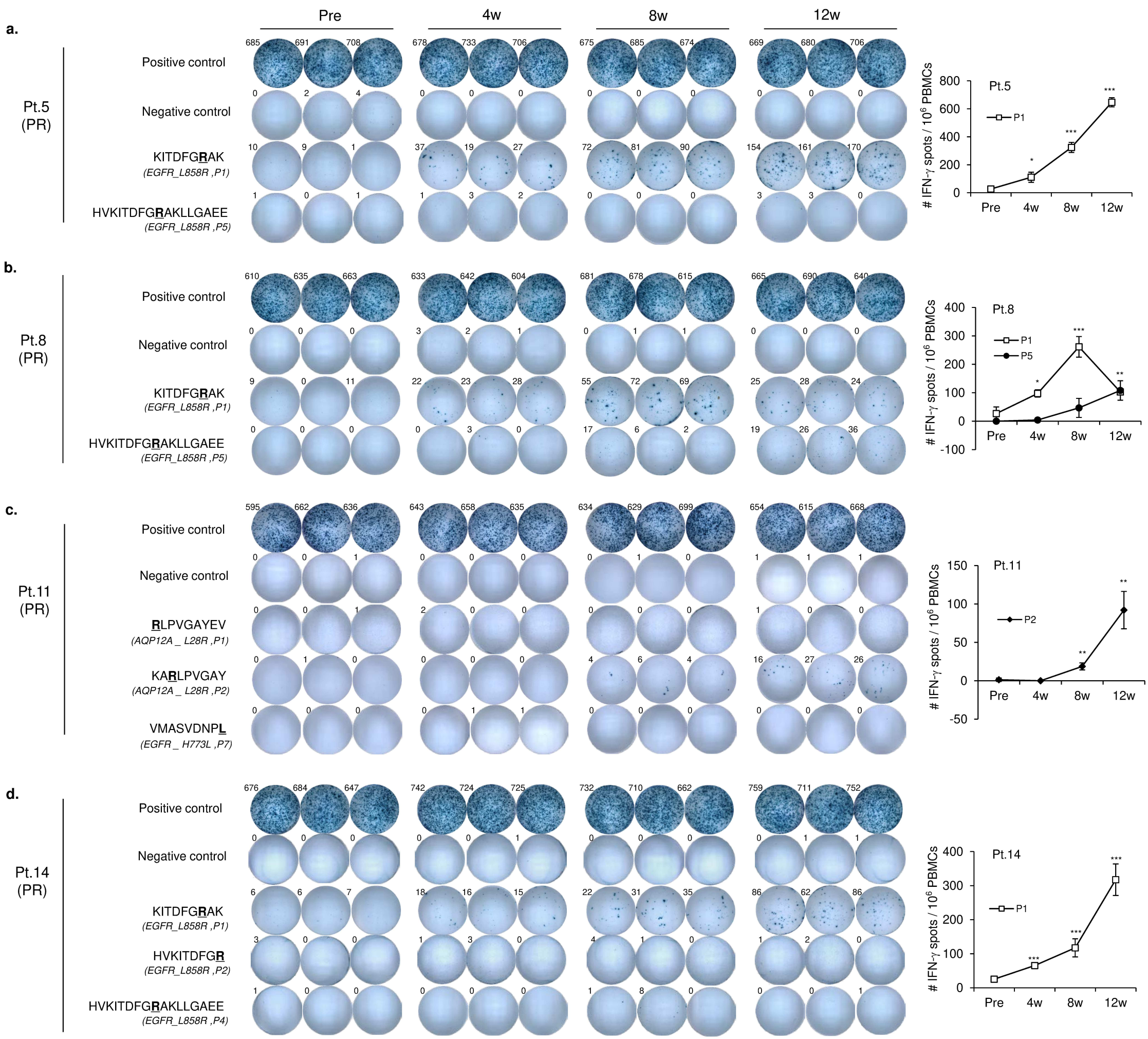

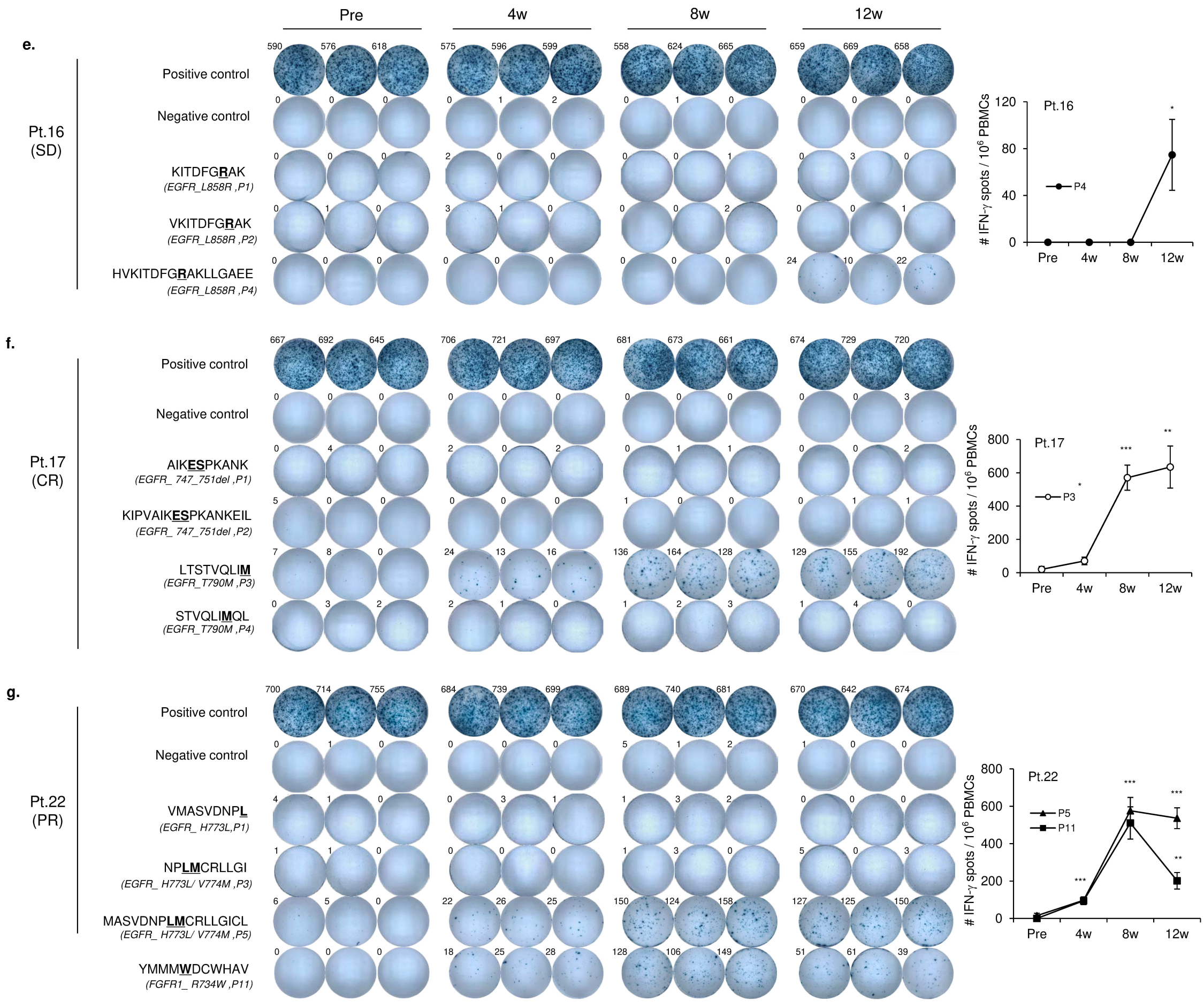

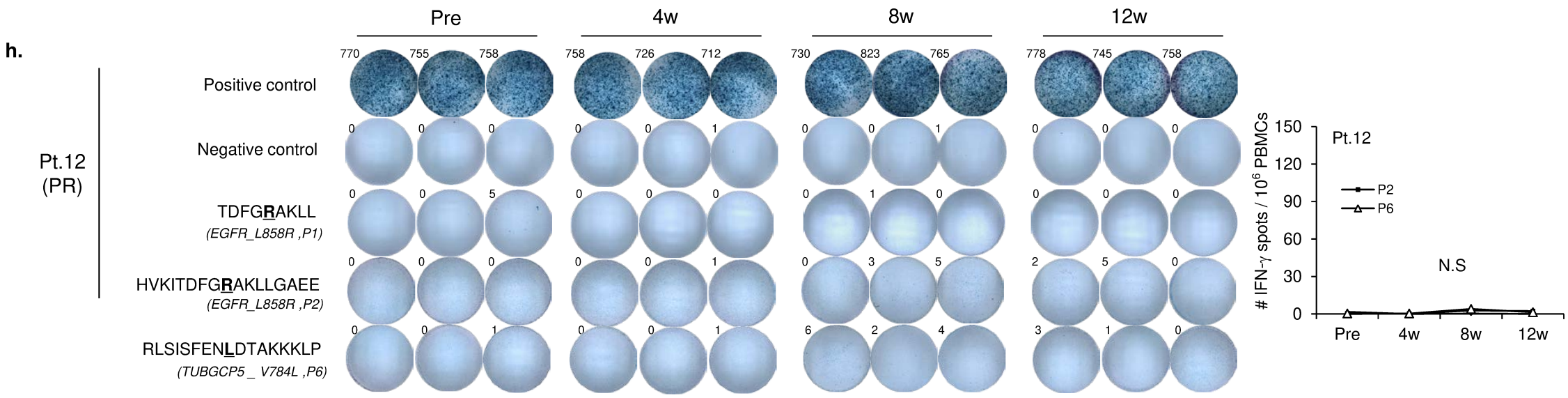

Fig. S7. ELISPOT-based *ex vivo* peripheral blood immune monitoring of vaccine-induced responses. IFN-γ ELISPOT assay results show PPV-induced immune reactivity against selected vaccine peptides (2.5X 10^5 cell per well) in eight immunized patients, including 7 clinical responders. The EGFR(L858R) NeoAg peptide KITDFGRAK elicited dominant IFN-γ responses in three different responding Pts. 5, 8, and 14 (**a, b, d**); however, no immune response could be detected against this vaccine peptide in SD Pt. 16 (**e**). Complete responding Pt. 17 generated a dominant immune response against the LTSTVQLIM NeoAg peptide containing the shared EGFR(T790M) mutation (**f**). Two additional PR patients generated $CD8^+$ T cell responses against private mutation-encoding NeoAgs: the AQP12A(L28R) peptide KARLPVGAY in Pt. 11 (**c**) and the FGFR1(R734W) peptide YMMMWDCWHAV in Pt. 22 (**g**). Immune responses against long, $CD4^+$ restricted EGFR NeoAg peptides were also elicited in 3 of the patients: the EGFR(L858R)-containing peptide HVKITDFGRAKLLGAEE in Pts. 8 and 16 (**b, e**), and the H773L/V774M NeoAg peptide MASVDNPLMCRLLGICL in Pt. 22 (**g**). Also depicted are line graph summaries showing the number IFN-γ spots per 10^6 PBMC (normalized) for each vaccine peptide that elicited a response. Peptide identification numbers (P1, P2, etc.) correspond to those listed in Supplemental Table 2. Experiment was performed once in n=3 replicates. Data are mean ± SD. Statistical comparisons were measured compared to pre treatment. Two-tailed unpaired t test was used to analyze the statistical significance between groups. P<0.05 was considered significantly different. *P<0.05, **P<0.01, ***P<0.001.

a.

Mutation	MHC Allele	Peptide Sequence	HLA binding affinity (nM)	Vendor	Patients
EGFR_L858R	HLA-A*1101	KITDFGRAK	163	BCM, USA	Pt.5, Pt.8, Pt.14, Pt.16
EGFR_L858R	HLA-A*1101	VKITDFGRAK	644	BCM , USA	Pt.5, Pt.8, Pt.14, Pt.16
EGFR_L858R	HLA-A*3101	HVKITDFGR	10	BCM , USA	Pt.14
EGFR_747_751del	HLA-A*1101	AIKESPKANK	1479	BCM , USA	Pt.17
EGFR_746_750del	HLA-A*3001	AIKTSPKANK	1047	BCM , USA	Pt.3
EGFR_T790M	HLA-C*1502	LTSTVQLIM	584	MBL, Japan	Pt.17

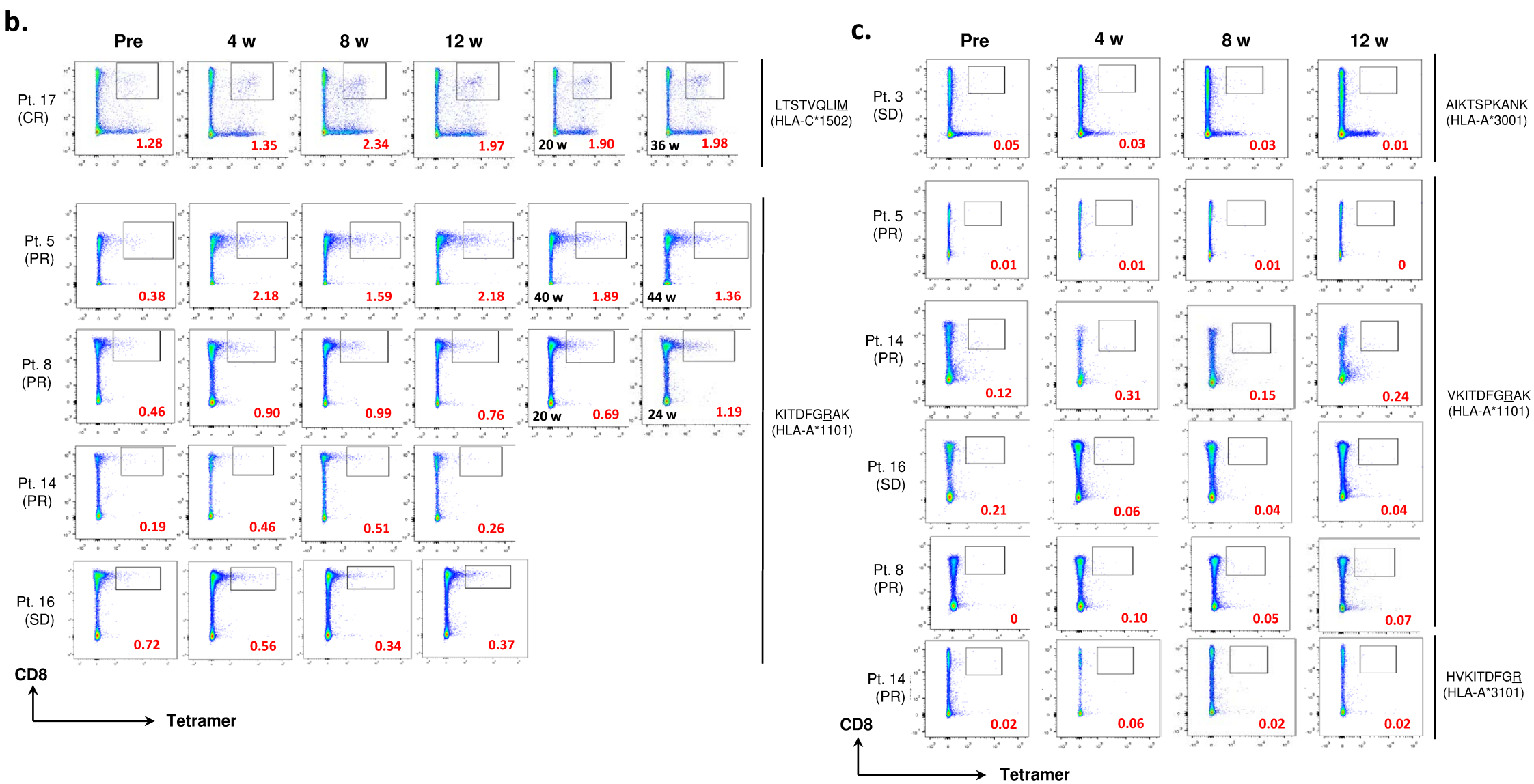

Fig. S8. HLA/peptide tetramer-based immune monitoring of vaccine-induced CD8⁺ T-cell responses. a. Listing of custom synthesized EGFR neoantigen tetramers used for immune monitoring analyses. **b, c.** Tetramer staining results of *ex vivo* pre- and post-vaccine PBMCs drawn at the time points indicated. **b.** EGFR neoantigen-specific CD8⁺ T cell populations were observed for PPV Pts. 5, 8, 14, and 16 (L858R) and 17 (T790M). **c.** Shown are examples of negative EGFR neoantigen tetramer staining of PBMC drawn from vaccinated Pts. 3, 5, 8, 14 and 16.

Fig. S9. HLA class I and class II superfamily peptide binding analysis of shared EGFR neoantigens. HLA binding prediction was performed for EGFR neoantigen peptides containing the 10 most prevalent EGFR mutations in lung cancer, including five shared point mutations (S768I, H773L, T790M, L858R, and L861Q) and five common Exon 19 deletions (legend). **a.** Number of 9, 10, or 11-mer EGFR neoantigen peptides predicted to bind to the 100 most prevalent HLA class I allotypes worldwide with predicted binding affinity of 500 nM or less. Allotypes are divided into HLA superfamilies, revealing distinct superfamily binding preferences for different shared EGFR mutations. **b.** Number of 9, 10, or 11-mer EGFR neoantigen peptides predicted to bind to HLA class I allotypes with predicted binding affinity of 5000 nM or less. **c.** Number of 17-mer EGFR neoantigen peptides predicted to bind to HLA class II allotypes with predicted binding affinity of 500 nM or less. Binding predictions were performed using NetMHCpan4.0 for HLA class I peptides and NetMHCII2.3 for HLA class II peptides. HLA class I and II superfamily groupings were adapted from references [25-27]. BX, unclassifed HLA-B allotypes.

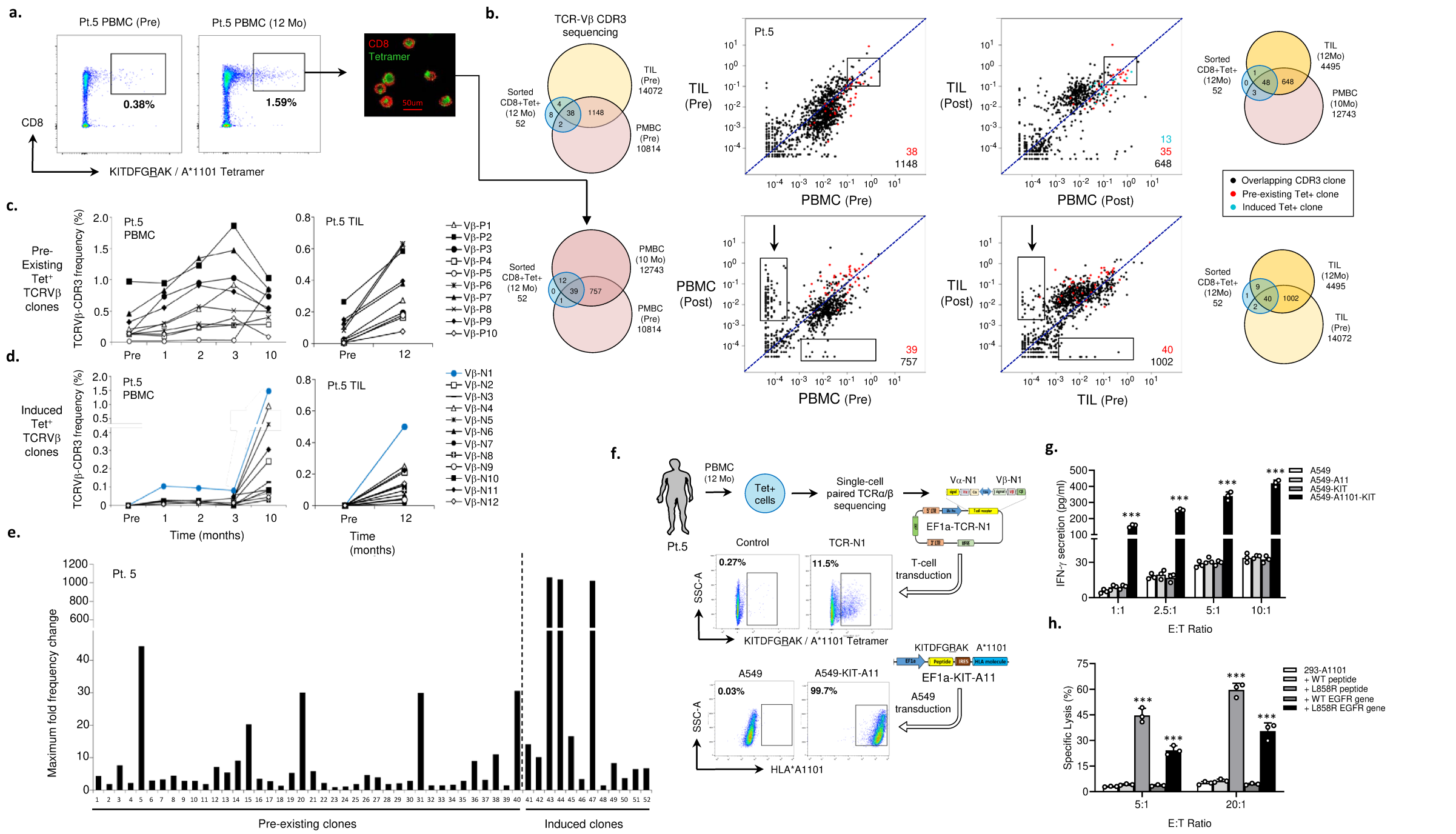

Fig. S10 Neoantigen vaccination induced increased frequencies and numbers of EGFR-L858R neoantigen-specific T cell clones in peripheral blood and tumor of Patient 5. a. HLA-A*1101/KITDFGRAK tetramer staining and flow sorting of CD8+Tetramer+ (Tet+) T cells from 10-month post-PPV PBMC of Patient 5. Sorted Tet+ cells underwent single-cell TCRa/b sequencing. **b.** TCRVβ-CDR3 sequencing was performed on Patient 5 PBMC and tumor biopsies taken pre- or post-PPV treatment. Venn diagrams and dot plots show the numbers and frequencies of CDR3 clones that overlap between pairs of samples. 52 high-confidence Tet+ Vβ-CDR3 clones sorted from post-PPV showed a high degree of overlap with both PBMC and TIL CDR3 clones (red dots). PPV induced significant increases in the frequency of neoantigen-specific Tet+ clones (small boxes), and 13 new Tet+ clones also appeared post-PPV (blue dots). Immunization also induced a population of other CDR3 clones in both PBMC and TIL (black arrows) **c.** PBMC and TIL frequencies of the top 10 pre-existing Tet+ CDR3 clones at time points prior to and post-PPV. **d.** PBMC and TIL frequencies of 12 vaccine-induced Tet+ CDR3 clones prior to and post-PPV. **e.** Maximum fold expansion of 52 Tet+ CDR3 clones in peripheral blood during the course of PPV treatment. Induced clones were not detectable in pre-treatment PBMC. **f.** Single-cell sequencing of sorted Tet+ clones facilitated cloning of Va-N1 and Vb-N1 with the HLA-A*1101/KITDFGRAK tetramer. A549 cells were also engineered to express HLA-A*1101 and/or a KITDFGRAK peptide-encoding minigene. **g.** Interferon-gamma ELISA results of TCR-N1 engineered T cells co-cultured with control parental A549, A549-A*1101, A549-KIT minigene, or A549-A*1101/KIT minigene-transduced target cells. Experiment was performed once in n=3 replicates. Data are mean ± SD. **h.** Specific ^{51}Cr release assay shows KITDFGRAK-specific TCR-T induced lysis of A*1101-transduced 293 target cells, before or after pulsing with WT EGFR peptide (KITDFGLAK) or mutated L858R EGFR peptide (KITDFGRAK), or following transduction with full-length wild-type or L858R mutant EGFR cDNA. Experiment was repeated twice independently and each experiment was performed in n=3 replicates. Data are mean ± SD. Statistical comparisons were measured compared to control. Two-tailed unpaired t test or Mann-Whitney U test was used to analyze the statistical significance between groups. $P<0.05$ was considered significantly different. **, $P<0.01$; ***, $P<0.001$.

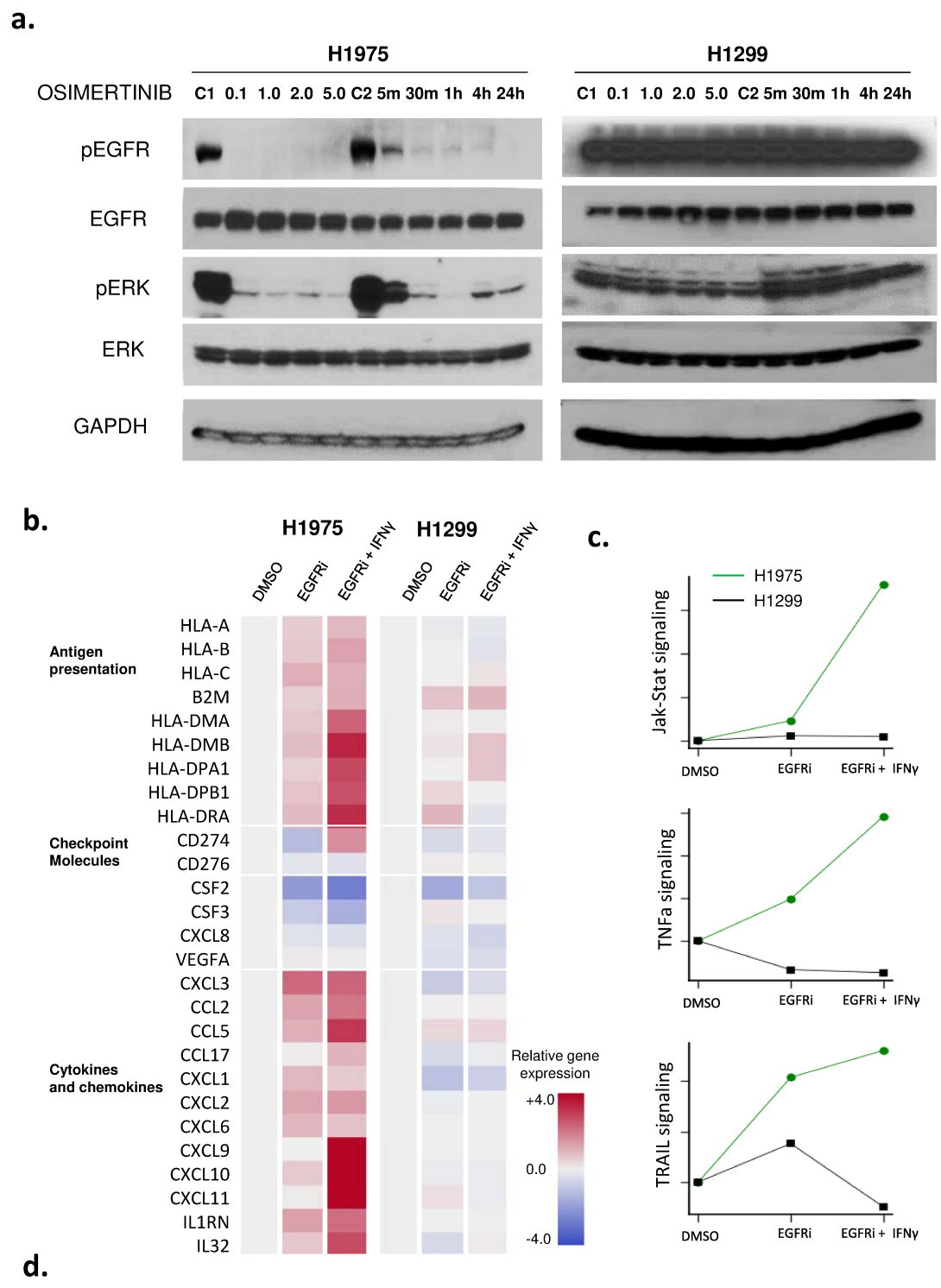

d.

Gene Set Name [# Genes (K)]	Description	# Genes in Overlap (k)	k/K	p-value	FDR q-value
HALLMARK_TNFA_SIGNALING_VIA_NFKB [200]	Genes regulated by NF-kB in response to TNF [GeneID=7124].	5		$8.88\ e^{-12}$	$4.44\ e^{-10}$
HALLMARK_IL6_JAK_STAT3_SIGNALING [87]	Genes up-regulated by IL6 [GeneID=3569] via STAT3 [GeneID=6774], e.g., during acute phase response.	3		$1.31\ e^{-7}$	$3.26\ e^{-6}$
HALLMARK_INFLAMMATORY_RESPONSE [200]	Genes defining inflammatory response.	3		$1.61\ e^{-6}$	$2.68\ e^{-5}$
HALLMARK_INTERFERON_ALPHA_RESPONSE [97]	Genes up-regulated in response to alpha interferon proteins.	2		$6.58\ e^{-5}$	$8.22\ e^{-4}$
HALLMARK_ALLOGRAFT_REJECTION [200]	Genes up-regulated during transplant rejection.	2		$2.79\ e^{-4}$	$2\ e^{-3}$
HALLMARK_IL2_STAT5_SIGNALING [200]	Genes up-regulated by STAT5 in response to IL2 stimulation.	2		$2.79\ e^{-4}$	$2\ e^{-3}$
HALLMARK_INTERFERON_GAMMA_RESPONSE [200]	Genes up-regulated in response to IFNG [GeneID=3458].	2		$2.79\ e^{-4}$	$2\ e^{-3}$

Fig. S11 **a.** EGFR inhibitor Osimertinib treatment of H1975 (EGFR-L858R/T790M) and H1299 (EGFR-WT) lung cancer cells showed significantly decreased phospho-EGFR and phospho-ERK in H1975 cells as shown by Western blot. EGFRi concentration in uM is shown. C1 and C2 are untreated control cells. **b.** Heat map showing RNA transcript changes in H1975 and H1299 cells following exposure to EGFRi (24h) or EGFR (24h) plus IFN-γ (12h). **c.** Gene signature changes in Jak-Stat, TNFα, and TRAIL signaling following EGFRi or EGFRi+IFNγ treatment. **d.** Gene set enrichment analysis of RNAseq following EGFRi treatment of H1975 cells.